Life Sciences 250 (2020) 117578

Contents lists available at ScienceDirect

Life Sciences

journal homepage: www.elsevier.com/locate/lifescie

RYBP inhibits esophageal squamous cell carcinoma proliferation through downregulating CDC6 and CDC45 in G1-S phase transition process

Yue Ke, Wei Guo, Shan Huang, Yuxing Li, Yuyan Guo, Xiaoxiao Liu, Yingying Jin, Hongbing Ma*

Department of Radiation Oncology, Second Affiliated Hospital, Xi'an Jiaotong University, 710004 Xi'an, China

ARTICLE INFO

Keywords:
Esophageal squamous cell carcinoma
RYBP
Cell cycle
CDC6
CDC45

ABSTRACT

Aims: RING1 and YY1-binding protein (RYBP) is an epigenetic regulator and plays crucial roles in embryonic development. The anti-tumor effect of RYBP has been reported in several cancers recently, but the role of RYBP in esophageal squamous cell carcinoma (ESCC) has not been fully elucidated. The present study aimed to investigate the biological function and the underlying molecular mechanisms of RYBP in ESCC.

Materials and methods: We detected the expression of RYBP in ESCC tissue microarrays (TMA) by immunohistochemistry. Cell proliferation was assessed by CCK8 and colony formation assays. Cell cycle was analyzed by flow cytometry. Gene expression was determined by transcriptome arrays, quantitative real-time PCR (qRT-PCR) and Western blot. Four-week-old male nude mice were used to evaluate the effect of RYBP in ESCC growth.

Key findings: We found that RYBP was downregulated in ESCC compared with adjacent normal tissues. A high level of RYBP expression predicted a better outcome of ESCC patients. Furthermore, overexpression of RYBP inhibited ESCC growth both in vitro and in vivo. Transcriptome arrays and functional studies showed that RYBP decreased the expression of genes related to cell cycles, especially CDC6 and CDC45, which were essential to initiate the DNA replication and G1-S transition.

Significance: Taken together, our study suggests that RYBP suppresses ESCC proliferation by downregulating CDC6 and CDC45, thus inhibiting the G1-S transition.

1. Introduction

Esophageal cancer is one of the most common and lethal malignant tumors worldwide [1]. The major pathological type in China is esophageal squamous cell carcinoma (ESCC), which accounts for > 90% of esophageal cancer. Due to the lack of typical symptoms and sensitive screening methods, most cases are diagnosed at an advanced or terminal stage. Although the combination of surgery, radiotherapy, and chemotherapy becomes a standard treatment strategy, the prognosis remains poor. Currently, the 5-year survival rate of esophageal cancer is 10% to 15% [2]. Therefore, the study of molecular mechanisms and search for new drug therapeutic targets are needed [3,4].

The RYBP was first identified as a protein interacting with RING1, an E3-ubiquitin ligase [5]. Functionally, RYBP plays an essential role in embryonic development through epigenetic mechanisms, such as the differentiation of embryonic stem cells, cardiomyocytes, and neurons [6–8]. RYBP is recognized as one of the epigenetic factors because of its ability to interact with polycomb group (PcG) and trithorax group (trxG), which serve as an epigenetic silencing factor and epigenetic activating factor, respectively [9]. Besides, RYBP was found to regulate apoptosis by interacting with cell death-related proteins. Several studies showed that a high level of RYBP could induce apoptosis. Mechanically, RYBP promotes cell death through Fas-mediated apoptosis by interacting with FADD, Caspase8, −10 and enhancing death-inducing signaling complex (DISC) formation. Also, RYBP interacts with DED-containing DNA-binding protein (DEDD) and promotes its relocalization from the cytoplasm to the nucleus [10]. Moreover, RYBP can interact with FANK1 and Apoptin and specifically induce tumor-associated apoptosis [11,12].

Recent studies proposed an anti-cancer function of RYBP in HCC [13–16], lung cancer [17–19], prostate cancer [20–22], breast cancer [23–25], cervical cancer [26,27], glioblastoma [28,29], and ileal carcinoid [30,31]. Gene dosage alterations on 3p12–14 predict poor outcomes in cervical cancer patients, and RYBP was supposed to be one of the candidate target genes [26,27]. The data from the cancer genome atlas (TCGA) showed that RYBP expression of glioblastoma patients was decreased by 49.3% compared with healthy tissue [32]. Besides, a high level of RYBP is correlated with a better prognosis of HCC and NSCLC.

* Corresponding author.
E-mail address: mhbxian@126.com (H. Ma).

https://doi.org/10.1016/j.lfs.2020.117578
Received 13 December 2019; Received in revised form 18 March 2020; Accepted 18 March 2020
Available online 21 March 2020
0024-3205/

RYBP inhibits HCC and NSCLC cell growth and promotes apoptosis through interacting with Bax, PARP-1, and Caspase 8 [13,19]. However, the role of RYBP in ESCC has not been elucidated.

In this study, we found that RYBP expression was decreased in ESCC tumor tissue s with the adjacent tissue. High expression of RYBP predicted a good outcome for ESCC patients. We further explored the biological function and underlying mechanisms of RYBP in ESCC through overexpressing RYBP and transcriptome array analysis. Our results suggest that RYBP may suppress ESCC cell proliferation by decreasing CDC6 and CDC45, thus inhibiting the G1-S phase transition.

2. Material and methods

2.1. Cell lines and culture

Human ESCC cell lines KYSE30, KYSE140, KYSE150, KYSE170, KYSE180, KYSE410, KYSE510 were obtained from Dr. Yutaka Shimada at the Hyogo College of Medicine [33]. Eca-109 cell line was purchased from the Cell Resource Center of Shanghai Institute of Life Sciences, Chinese Academy of Sciences (Shanghai, China). All cell lines were incubated in RPMI-1640 or DMEM with 10% fetal bovine serum at 37 ˚C in 5% CO_2.

2.2. Plasmids transfection and lentivirus infection

The plasmids of RYBP, pCMV6, CDC6, and CDC45 were purchased from Origene (Rockville, MD, USA). Transfection was carried out using Lipofectamine 2000 (Invitrogen, Carlsbad, CA, USA) according to the manufacturer's instructions. Cell lines were selected by G418 sulfate (Promega, Madison, WI, USA), as described previously [34]. Lentivirus of RYBP and control were obtained from GeneChem Corporation (Shanghai, China). Cells were seeded into 96-well plates and infected with lentivirus according to the manufacturer's instructions. 72 h after infection, cells were selected with puromycin (1 μg/ml for KYSE170 cell line and 2 μg/ml for Eca-109 cell line).

2.3. Western blotting

ESCC cells were lysed with Ripa buffer containing protease inhibitors (Hat Biotechnology, Xi'an, China). The proteins were quantified by the BCA protein assay kit (Hat Biotechnology, Xi'an, China). 30 μg proteins were separated by 8–12% SDS-PAGE and transferred to a polyvinylidene difluoride (PVDF) membrane (Thermo Fisher Scientific, MA, USA). The membranes were then blocked with 8% skim milk for one hour at room temperature followed by incubating with the following primary antibodies, rabbit anti-human RYBP antibody (ab5976, 1:1000, Abcam, Cambridge, MA, USA), rabbit anti-human MCM3 antibody (ab128923, 1:1000, Abcam, Cambridge, MA, USA), rabbit anti-human MCM5 antibody (ab75975, 1:1000, Abcam, Cambridge, MA, USA), rabbit anti-human CDC6 antibody (ab109315, 1:1000, Abcam, Cambridge, MA, USA), rabbit anti-human CDC45 antibody (ab126762, 1:1000, Abcam, Cambridge, MA, USA), rabbit anti-human Flag antibody (#14793, 1:1000, Cell Signaling Technology, Danvers, MA, USA) and mouse anti-human actin antibody (A5441, 1:3000, Sigma-Aldrich, St. Louis, MO, USA). The membranes were then washed and incubated with the secondary antibody, anti-rabbit IgG(#7074, 1:10000), and anti-mouse IgG (#7076, 1:10000) antibodies conjugated with HRP (Cell Signaling Technology, Danvers, MA, USA). The protein immunoreactive signals were detected by exposure to X-ray film. The integrated density of each band was measured, and subtracted the background levels by Image J software (National Institutes of Health, Bethesda, MD), and quantified by normalization to the expression of β-actin.

2.4. Colony formation assay and CCK8 assay

For colony formation assay, 200 cells per well were plated into 6-well plates and cultured for ten days. Afterward, cells were fixed with 4% paraformaldehyde, stained with crystal purple for 10 min, and counted as described previously [35]. For CCK8 assay, 1000 cells per well were seeded in 96-well plates, CCK8 (Wobisen, Beijing, China) was used to assess the cell growth every day through microplate reader (Bio-rad, Hercules, CA, USA) at 450 nm wavelength.

2.5. Cell cycle analysis

The cell cycle was measured by using flow cytometry and the detection reagent kit (KeyGEN Biotech, Jiangsu, China) according to the manufacturer's instructions. Briefly, 2×10^6 Cells were seeded in 6-well plates and cultured for 24 h. Afterward, cells were collected by trypsin (Invitrogen), washed with PBS (centrifuged with 800 rpm for 5 min) three times, and fixed in 70% ice-cold ethanol at 4 ˚C overnight. After washing with ice-cold PBS (centrifuged with 1500 rpm for 5 min) twice, cells were stained with 500 μl propidium iodide containing RNase A buffer for 30 min away from light. The percentage of cells were calculated and analyzed by flow cytometry (BD Biosciences, Franklin Lakes, NJ, USA).

2.6. Microarray analysis

The Affymetrix Human HTA2.0 (OE Biotech, Shanghai, China) was used to analyze gene expression alteration after transfecting plasmids of RYBP or pCMV6 in KYSE170 cell lines. Affymetrix GeneChip Command Console (version 4.0, Affymetrix) software and Expression Console (version1.3.1, Affymetrix) software were used to extract raw data and offer RMA normalization for both gene and exon-level analysis, respectively. GeneSpring software (version 12.5; Agilent Technologies) was used for the basic analysis. Differentially expressed genes were then identified through fold change as well as P value calculated with Student's *t*-test. The threshold set for up- and down-regulated genes was a fold change≥ 2.0 and a P value≤ 0.05. Afterward, GO analysis, KEGG analysis, and Hierarchical Clustering were performed.

2.7. Quantitative RT-PCR

Total RNA was extracted by TRIzol reagent (Invitrogen, Carlsbad, CA, USA) according to the manufacturer's protocol. Then 1 μg of total

Table 1
The primers used for Q-PCR.

POLD2	Forward: 5'-CCACCCGCCTCATCCAAAT-3′ Reverse: 5'-CCAAGACCAGCTCGTCATCTG-3′
PCNA	Forward: 5'-ACACTAAGGGCCGAAGATAACG-3′ Reverse: 5'-ACAGCATCTCCAATATGGCTGA-3′
FEN1	Forward: 5'-CACCTGATGGGCATGTTCTAC-3′ Reverse: 5'-CTCGCCTGACTTGAGCTGT-3'
MCM3	Forward: 5'-GGCCTCCATTGATGCTACCTA-3' Reverse: 5'-ACTTTGGGACGAACTAGAGAACA-3'
MCM5	Forward: 5'-AGCATTCGTAGCCTGAAGTCG-3' Reverse: 5'-CGGCACTGGATAGAGATGCG-3'
RFC3:	Forward: 5'-ATTGGGAGGTGTATCTGAGGG-3' Reverse: 5'-CTTCCACGAACTTCAAGGAGC-3'
RFC5:	Forward: 5'-ACTCCTGAACTCATGGTTCCC-3' Reverse: 5'-CCCTACGCATGTCTCCACT-3′
POLA1	Forward: 5'-AAAGATCCATTGGAGCTTCACC-3' Reverse: 5'-TCAGCACGTTTAAGAGGAACAG-3′
POLA2:	Forward: 5'-AGGAGCTAGAGACATTGTTTCCA-3' Reverse: 5'-CTCGCTTCTGAGAACCCTTTG-3′
CCNE2:	Forward: 5'-TCAAGACGAAGTAGCCGTTTAC-3' Reverse: 5'-TGACATCCTGGGTAGTTTTCCTC-3′
CDC7:	Forward: 5'-AGTGCCTAACAGTGGCTGG-3′ Reverse: 5'-CACGGTGAACAATACCAAACTGA-3′
CDK1:	Forward: 5'-GGATGTGCTTATGCAGGATTCC-3' Reverse: 5'-CATGTACTGACCAGGAGGGATAG-3′
GAPDH:	Forward: 5'-GCTGAGAACGGGAAGCTTGT-3′ Reverse: 5'-GCCAGGGGTGCTAA GCAGTT-3'

RNA was reverse transcribed into cDNA using a Reverse Transcription kit (Takara Bio Inc., Kusatsu, Japan). The cDNA was used for Q-PCR analysis on an iCycler iQ5 Real-Time PCR detection system (BioRad) following the manufacturer's protocol. The expression of the target gene was normalized to *Gapdh*. The primers used for Q-PCR are shown in Table 1.

2.8. Immunohistochemistry staining (IHC)

Tumor tissues were fixed with 4% paraformaldehyde for 16 h, and 10 μm sections were prepared. Then the sections were blocked with PBS containing 10% normal goat serum and incubated with the specific antibodies at 4 °C overnight. Images were obtained on a Slide scanning electron microscope (Carl Zeiss, Oberkochen, Germany).

The ESCC tissue microarrays (TMAs) were purchased from Outdo Biotechnology Corporation (Shanghai, China), Eso-Squ180Sur-01, and incubated with a rabbit anti-human RYBP antibody (1800) overnight. The results were assessed independently by two pathologists based on the intensity and the percentage of RYBP-positive cells. The intensity of the staining was scored as 0 (negative), 1 (weakly positive), 2 (moderately positive), and 3 (strongly positive). The extent of expression was categorized as 1 (stained cells: 1–10%), 2 (11–50%), 3 (51–80%), 4(80–100%). The intensity score and distribution score were then multiplied to attain a total score. The score which was equal to or exceeded six was identified as high-expression, and the score below six was identified as low-expression. Written informed consent was obtained from the patients, and the protocol was approved by the Ethical Review Board of Taizhou Hospital of Zhejiang province (approval number 717–1428, date of approval 2010-01-26).

2.9. ESCC xenografts

All animal experiments were performed according to the guidelines approved by the Animal Care and Use Committee of the Laboratory Animal Center of Xi'an Jiaotong University (approval number 2018–2191, date of approval 2018-02-26). All studies involving animals were reported according to the ARRIVE guidelines. Four-week-old male nude mice with similar weigh (16 ± 1.5 g) were purchased from the Laboratory Animal Center (Xi'an Jiaotong University, China) randomly divided into an experimental or control group. Two groups (three mice per group, three mice per cage) of mice were housed in the special pathogen-free (SPF) laboratory under standard conditions. After acclimation for one week, 1×10^6 cells of KYSE170-RYBP or KYSE170-Ctrl cells were injected subcutaneously at the right flank to establish ESCC tumors models. Tumors volume and the weight of mice were measured every three days. Tumor volume was calculated using the

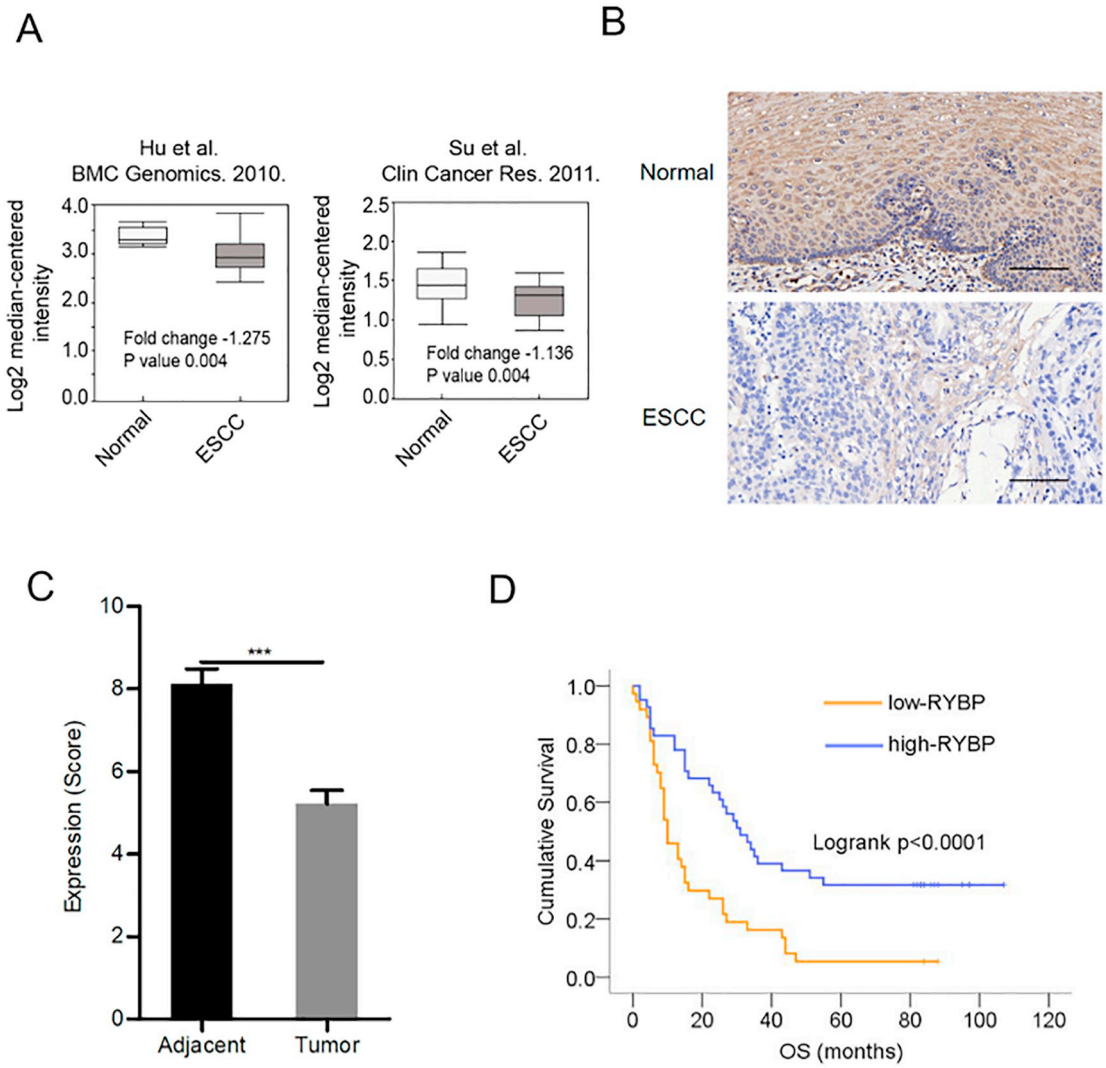

Fig. 1. The expression of RYBP in ESCC and adjacent tissues. (A) The levels of RYBP in ESCC and adjacent tissues in studies referred to the Oncomine database. (B) Representative RYBP IHC images in TMAs and (C) expression scores were quantified in adjacent tissues (n = 63) and tumor (n = 80) samples. (D) Kaplan-Meier survival curves of the ESCC patients with high and low expression of RYBP. The scale bars indicate 100 μm (B). ***P < 0.001.

formula $a*b^2$ (a = long diameter, b = short diameter). Thirty-six days later, mice were anaesthetized with pentobarbital sodium (40 mg/kg, intraperitoneal injection) and sacrificed by cervical dislocation. Tumors were stripped and photographed.

2.10. Statistical analyses

All experiments were performed and repeated at least three times. Data were presented as mean ± SD. Statistical analyses were calculated by SPSS 22.0 (SPSS, Inc., Chicago, IL, USA) and GraphPad Prism 7.0 (GraphPad Software, Inc., San Diego, CA, USA). The differences between the two groups were compared through the Student's *t*-test or Mann-Whitney *U* test. A Log-rank test was used to analyze the significance of Kaplan-Meier curves. A multivariate analysis was performed using a Cox multivariate proportional hazard regression model in a stepwise manner (Forward: LR). A P value < 0.05 was considered statistically significant.

3. Result

3.1. RYBP is downregulated in human ESCC tissue, and low expression of RYBP predicts poor prognosis in ESCC patients

Several studies showed that RYBP was down-expressed in various tumor tissues. To determine whether RYBP expression altered in ESCC tissues, we first referred to the Oncomine database [36]. Two studies, based on 17 [37] and 53 [38] pairs of matched normal and ESCC samples, respectively, showed that RYBP was significantly downregulated in ESCC samples compared to the corresponding adjacent tissues (Fig. 1A). Next, we analyzed the expression of RYBP in 80 human ESCC samples by immunohistochemistry staining. We found that the level of RYBP significantly decreased in ESCC compared to adjacent normal tissues (Fig. 1B—C). Specifically, 91.25% of the cases (73/80) were RYBP positive, among which 40% (32/80) showed weak intensity, 36.25% (29/80) moderate intensity, and 15.00% (12/80) strong intensity. However, 100% (63/63) of the corresponding adjacent normal tissues were RYBP positive. Only 7 cases, 11.1% (7/63) were weak intensity, 52.38% (33/63) moderate intensity, and 36.51% (23/63) strong intensity. Furthermore, we found that ESCC patients with low RYBP expression showed a significant decrease in overall survival (Fig. 1D). The association between RYBP levels and clinicopathological features was analyzed and summarized in Table 2. Univariate and multivariate analyses showed that the RYBP level was an independent prognostic factor of OS for ESCC patients (Table 3). Together, these data indicate that RYBP is downregulated in ESCC tissue, and low expression of RYBP predicts poor prognosis in ESCC patients.

Table 2
The association between RYBP levels and clinicopathological features in TMAs.

		Low	High	χ2	P value
		n = 37	*n* = 41		
Gender				3.627	0.057
	Male	32	28		
	Female	5	13		
Age,years				2.519	0.112
	≤65	22	17		
	> 65	15	24		
Differentiation				4.548	0.103
	High	5	1		
	Moderately	26	28		
	Low	6	12		
Vascular invasion				0.249	0.618
	Yes	36	39		
	No	1	2		
T stage				0.94	0.332
	T1T2	5	9		
	T3T4	32	32		
N stage				0.264	0.607
	N0	28	33		
	N1–3	9	8		
TNM stage				3.335	0.068
	I-II	14	24		
	III-IV	23	17		

Table 3
Univariate and multivariate analyses of the prognosis factors associated with overall survival in ESCC patients.

	Univariate		Multivariate	
	HR	P	HR(95%CI)	P
Gender(male vs female)		0.026		0.247
Age,years (≤65 vs > 65)		0.751		
Differentiation (I vs II vs III)		0.946		
Vascular invasion (Negative vs Positive)		0.252		
T stage (1, 2 vs 3, 4)		0.016		0.107
N stage (Negative vs Positive)		0.002	0.464(0.261–0.823)	0.009
TNM stage (I, II vs III, IV)		0.001		0.184
RYBP (high vs low)		0.000	0.428(0.256–0.714)	0.001

3.2. RYBP overexpression suppressed ESCC cell proliferation in vitro

To study the biofunction of RYBP in ESCC, we took advantage of ESCC cell lines. We observed that 4 of 8 tested cell lines barely expressed RYBP (KYSE30, Eca-109, KYSE150, KYSE170) and there was mild expression of RYBP in KYSE410 and 510, whereas the rest showed relatively higher RYBP expression (KYSE180 and KYSE140) (Fig. 2A), which was further indicative of the downregulation of RYBP in ESCC. Then, we constructed RYBP overexpression cell lines by using KYSE170 and Eca-109 (Fig. 2B) because they didn't express RYBP. Both CCK8 assay (Fig. 2C) and colony formation assay (Fig. 2D) showed that RYBP overexpression inhibited ESCC cell growth. Moreover, high level of RYBP significantly increased the proportion of cells in the G1 phase and decreased the proportion of cells in the S phase in both cell lines (Fig. 2E), suggesting the arrest of G1-S transition. Besides, we observed a decrease of the cells in the G2/M phase in KYSE170 but not Eca-109 cells, showing that the impact of RYBP on cell cycle might be different in these two cell lines. These results indicate that RYBP suppressed ESCC cell proliferation by inhibing G1-S phase transition.

3.3. Gene expression alteration in RYBP overexpression cell line

To study the underlying mechanisms by which RYBP suppressed ESCC cell proliferation and inhibited G1-S phase transition, we performed the Human Transcriptome Array 2.0 analysis. There were overall 559 differentially expressed genes induced by RYBP overexpression, among which 205 were upregulated and 354 were downregulated (Fig. 3A). KEGG analysis indicated that RYBP overexpression had significantly downregulated the DNA replication, cell cycle, and mismatch repair pathways (Fig. 3B—C Supplementary Table 1). Among these pathways we identified some important genes associated with DNA replication, such as CDC6, CDC45, MCM3 and MCM5, all of which are required for DNA replication and play important roles in the activation and maintenance of the checkpoint mechanisms in the cell cycle. For example, CDC6 is an essential licensing regulator for DNA replication because it contributes to the assembly of pre-replicative complexes (pre-RC) at origins to initiate DNA replication in G1 phase. We further confirmed the downregulation of several selected genes after RYBP overexpression by Q-PCR (e.g., CDC6, CDC45, MCM3, MCM5, et al.) (Fig. 3D). These findings suggest that RYBP inhibits ESCC cell proliferation through regulating the cell cycle.

3.4. RYBP inhibited ESCC through downregulating CDC6 and CDC45 in the G1-S transition process

Our results showed that the upregulation of RYBP significantly suppressed cell cycle of ESCC cells and decreased the levels of CDC6, CDC45, MCM3, and MCM5. Because CDC6 and CDC45 are essential proteins for the initiation of DNA replication, especially in the G1-S transition process, together with MCMs. Therefore, we proposed that RYBP may inhibit G1-S transition via the downregulation of these critical proteins. We first determined their protein levels after RYBP overexpression. RYBP slightly downregulated MCM3 and MCM5 both in KTSE170 and Eca-109 cells. However, we observed a dramatic decrease in CDC6 and CDC45 in Eca-109, but not KYSE170 cells (Fig. 4A). Due to these findings, we overexpressed CDC6 and CDC45 in RYBP overexpression cell lines to observe their influence on ESCC cell proliferation and cell cycle (Fig. 4B, 5A). In contrast to RYBP overexpression, CDC6 or CDC45 overexpression significantly promoted cell proliferation (Fig. 4C, 5B) and the G1-S transition process (Fig. 4D, 5C). Taken together, our results suggest that RYBP may suppress ESCC proliferation by downregulating CDC6 and CDC45, thus inhibiting the G1-S transition.

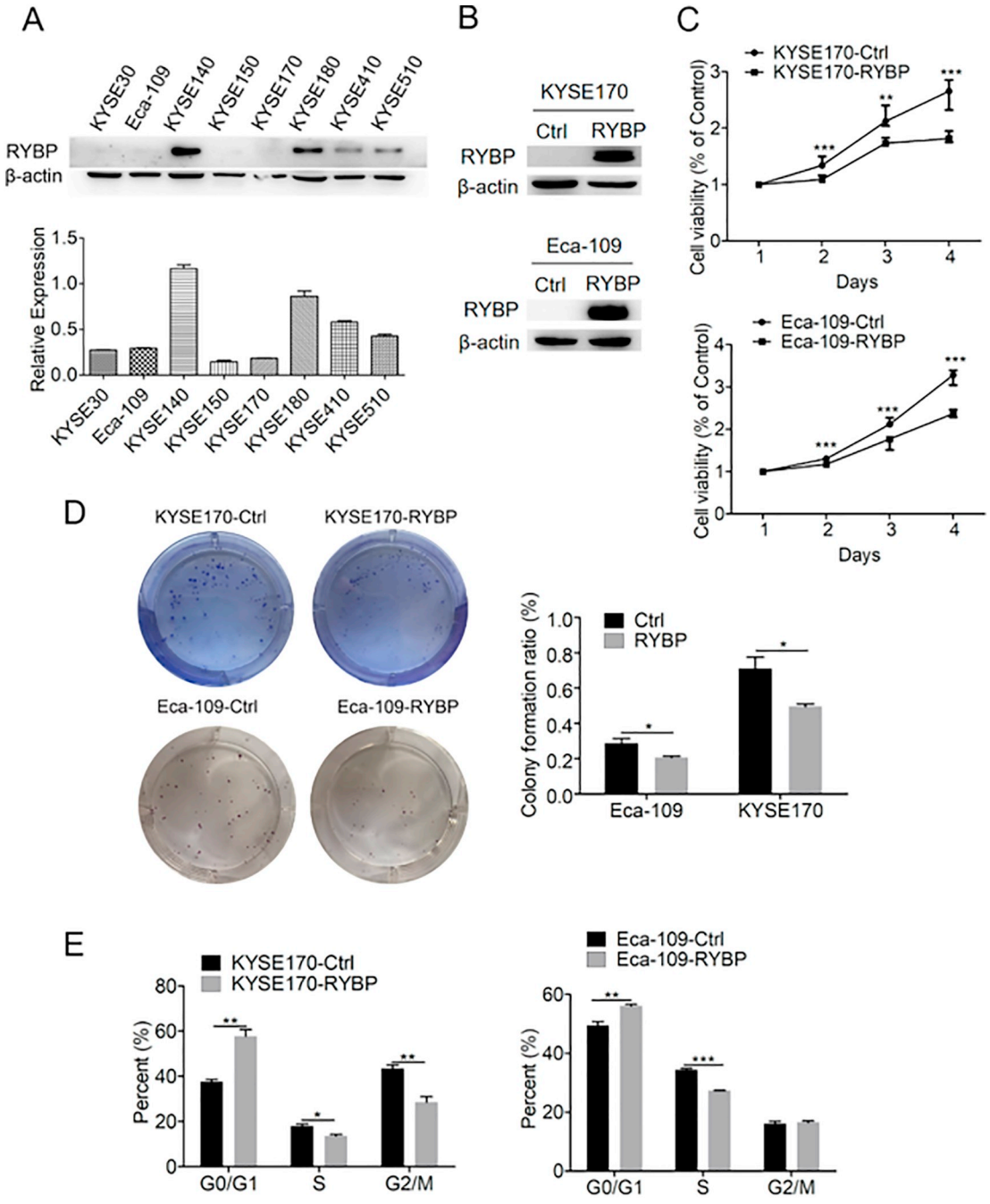

Fig. 2. High level of RYBP inhibits proliferation in ESCC lines. (A) RYBP expression in eight ESCC cell lines was determined and the quantification was shown by normalization to the expression of β-actin accordingly (mean ± SD), the experiment was conducted three times. (B) Overexpression of RYBP in KYSE170 and Eca-109 cell lines. (C) CCK8 cell proliferation and (D) colony formation assay after RYBP overexpression. (E) Cell cycle distribution was analyzed in both cell lines. *P < 0.05, **P < 0.01, ***P < 0.001.

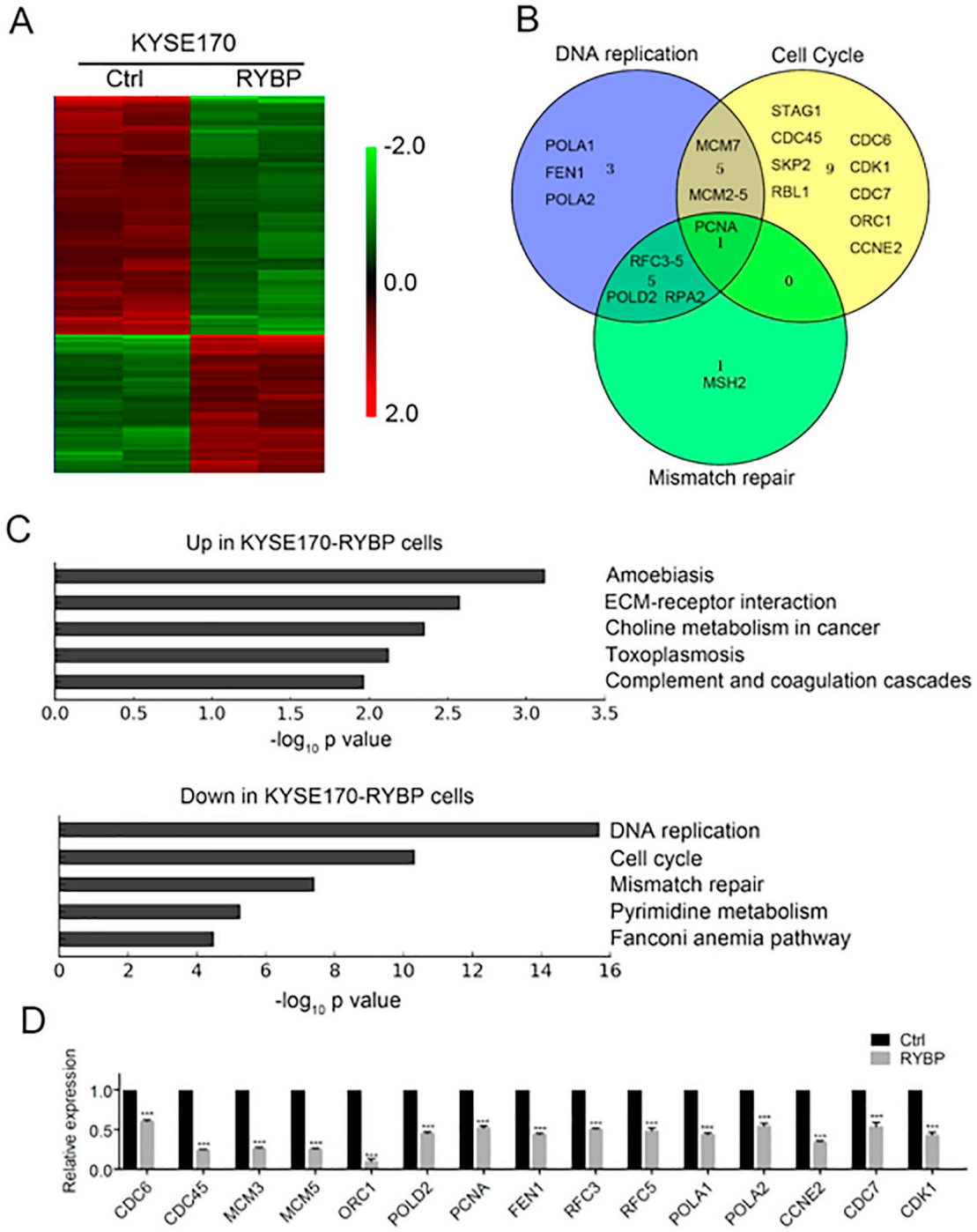

Fig. 3. Gene expression alteration in the RYBP overexpression cell line. (A) Clustering of the microarray data between the RYBP overexpression group and the control group. (B) Venn diagram showed the altered genes in DNA replication, cell cycle, and mismatch repair pathways. (C) KEGG pathway analysis of differentially expressed genes after RYBP overexpression. (D) The mRNA levels of candidate genes. The data represent the mean ± SD of relative mRNA levels versus control cells. ***P < 0.001.

3.5. RYBP inhibits ESCC tumor growth in vivo

Finally, we examined the inhibition potential of RYBP in vivo. The mice were four-week-old with similar weight (16 ± 1.5 g) before we inoculated KYSE170-RYBP or KYSE170-Ctrl cells. No mouse died from adverse effects. The tumor volume was dramatically decreased in RYBP overexpression group ($P < 0.05$). (Fig. 6A-C). IHC staining confirmed the higher level of RYBP in the overexpression group (Fig. 6D). Altogether, these data indicated that RYBP inhibits ESCC tumor growth in the mouse models.

4. Discussion

RYBP is a member of epigenetic regulators, playing crucial roles in the embryonic development and regulation of transcription. Although mounting evidence suggests an anti-tumor function of RYBP in diverse cancers, its role in ESCC remains unknown. Here we showed that the expression of RYBP decreased significantly in ESCC compared with corresponding adjacent tissue. The low level of RYBP predicted poor outcomes of patients. Furthermore, we proved that RYBP inhibits the G1-S transition by downregulating CDC6 and CDC45, thus suppressing

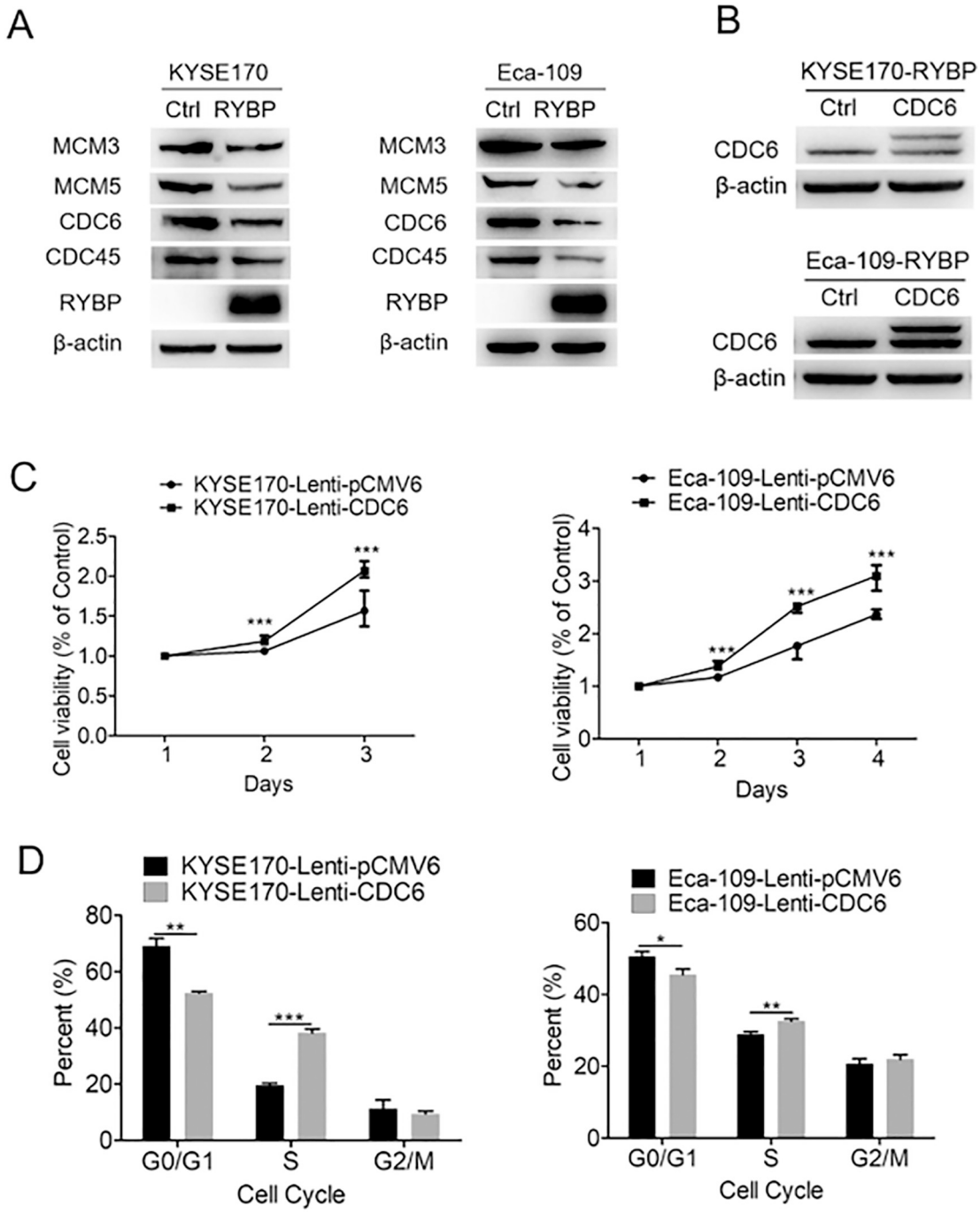

Fig. 4. RYBP inhibited ESCC proliferation through downregulating CDC6 in the G1-S transition process. (A) Expression of G1-S phase transition related proteins were detected in RYBP overexpression and control cells. (B) Overexpression of CDC6 in RYBP overexpression cell lines. (C) The relative cell viability was measured by CCK8. (D) Cell cycle distribution was determined in KYSE170 and Eca-109 cell lines. *P < 0.05, **P < 0.01, ***P < 0.001.

ESCC cell proliferation and exerting its anti-tumor function.

Previous studies showed that RYBP could inhibit HCC and NSCLC cell growth and promote their apoptosis through increasing Bax, PARP-1, and Caspase8 [13,19]. RYBP may also be involved in the progression and metastasis of breast cancer [25]. In our hand, we found that RYBP suppressed ESCC cell proliferation through inducing G1-S transition arrest. Transcriptomics profiling showed that genes related to DNA replication pathways were dramatically downregulated after RYBP overexpression. Many genes associated with cell cycle were identified, such as CDC6, CDC45, MCM3, and MCM5.

In our study, we showed that RYBP overexpression decreased the levels of CDC6, CDC45, MCM3, and MCM5, which are essential for the G1-S transition. The initiation of DNA replication is tightly controlled to ensure the precise genome duplication in every cell cycle. The mechanism of initiation is highly conserved, which composed of origin recognition, pre-replication (pre-RC) initiative complexes assembly, activation of helicase, and replisome loading [39]. CDCs and MCMs are essential proteins in the initiation of DNA replication. Studies showed that MCM complex is first loaded at replication origins mediated by CDC6 during G1 phase, and then converted to active CMG (CDC45, MCM, and GINS) helicase, which consist of CDC45, MCM2–7, and GINS during S phase [40]. Moreover, mounting evidence suggests that CDC6 and CDC45 are associated with tumor development. CDC6 was related to aggressive clinicopathological characteristics in bladder cancer and

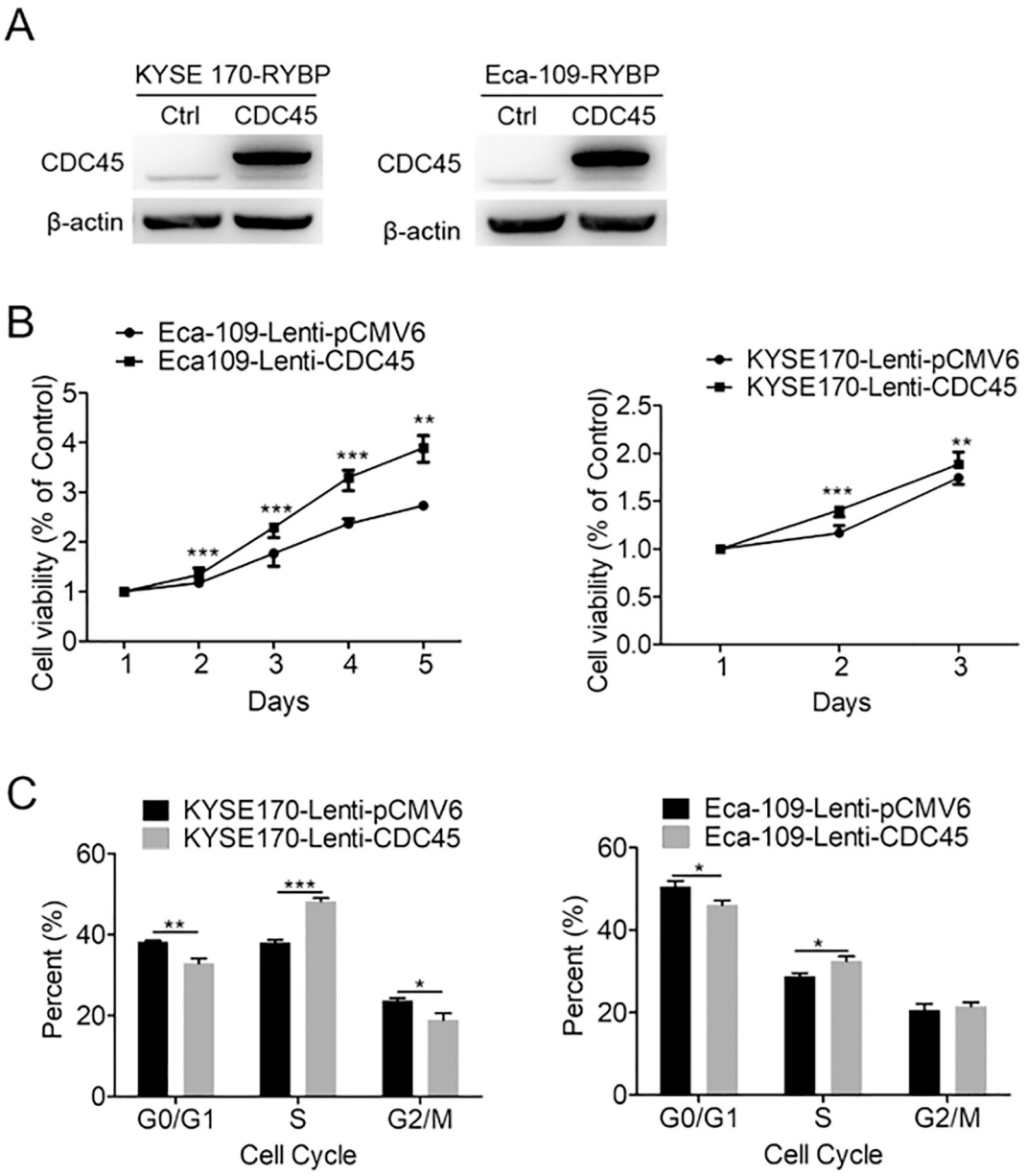

Fig. 5. RYBP inhibited ESCC proliferation through downregulatingCDC45 in the G1-S transition process. (A) Overexpression of CDC45 in RYBP overexpression cell lines. (B) The relative cell viability was measured by CCK8. (C) Cell cycle distribution was determined in KYSE170 and Eca-109 cell lines. *P < 0.05, **P < 0.01, ***P < 0.001.

prostate cancer, and downregulation of CDC6 sensitized bladder cancer cells to cisplatin [41,42]. Low expression of CDC6 suppresses tumorigenesis of osteosarcoma through upregulating p21 to promote apoptosis and downregulating Cyclin D1 and Cyclin A2 to induce G1 phase arrest [43]. In colorectal cancer (CRC), CDC6 and CDC45 expression were upregulated and significantly associated with the outcome of CRC patients [44].

RYBP has ubiquitin-binding activity and even could be itself ubiquitinated [45]. Currently, several proteins, such as FANK1, p53, MDM2, Ring1B, and UBE3A, were identified to be modulated by the ubiquitination-proteasome system (UPS) [11,46,47]. It has been reported that RYBP can interact with MDM2 and subsequently decrease MDM2-mediated p53 ubiquitylation, leading to the stabilization of p53 [46]. Besides, a ubiquitin-binding Npl4 zinc finger (NZF) domain of RYBP can preferentially recognize K63-ubiquitin chains, a property associated with some double-strand breaks (DSBs) repair proteins [48]. Moreover, the previous study found that RYBP mediated the YY1-E2Fs interaction, which controlled the CDC6 promoter activity in the G1/S phase [49]. However, the mechanism that RYBP downregulates CDCs remains largely unknown. We speculated that RYBP might promote the ubiquitylation-mediated degradation of CDCs, which needs further investigation.

Our study demonstrated that RYBP could downregulate CDC6 and CDC45, thus inhibiting DNA replication and suppressing ESCC cell proliferation.

5. Conclusion

In summary, our data suggested that RYBP exerts its anti-tumor effect by inhibiting G1-S transition. The high level of RYBP predicts a good outcome of patients with ESCC. RYBP may play as a biomarker for ESCC patients' outcomes.

Supplementary data to this article can be found online at https://doi.org/10.1016/j.lfs.2020.117578.

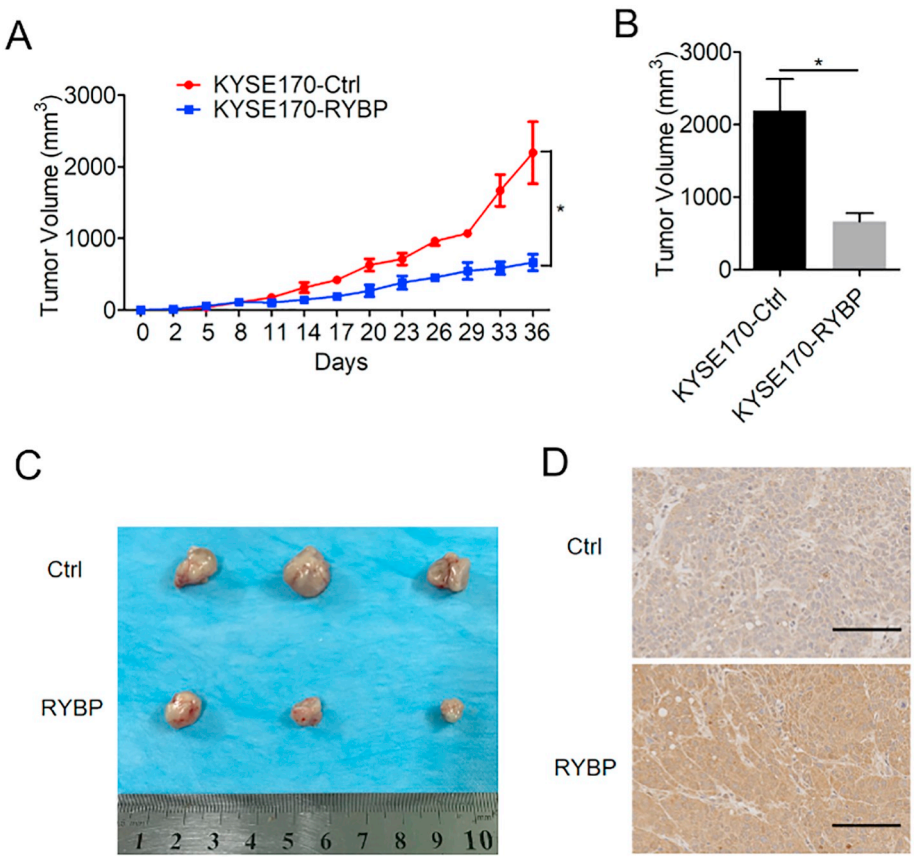

Fig. 6. RYBP overexpression inhibited ESCC growth *in vivo*. (A, B) KYSE170-Ctrl and KYSE170-RYBP cell lines were implanted into nude mice. Tumor volume was calculated at indicated time points. (C) Tumor appearance of the control tumor and the RYBP-overexpression tumor. (D) Representative RYBP IHC images of the control and RYBP-overexpression tumor. The scale bars indicate 100 μm. *P < 0.05.

Funding

This work was supported by the National Natural Science Foundation of China (2018-2191), Fund of General Project of Key Research and Development Plan of Shaanxi (2017SF-053), and Special Fund for talents of the Second Affiliated Hospital, Xi'an Jiaotong University (2018).

Conceived and designed the experiments: Yue Ke, Hongbing Ma. Performed the experiments and analyzed data: Yue Ke, Wei Guo, Yuxing Li, Yuyan Guo, Xiaoxiao Liu. Data collection: Yuyan Guo, Xiaoxiao Liu. Drafted the manuscript: Yue Ke. Revised the manuscript: Shan Huang, Yingying Jin.

CRediT authorship contribution statement

Yue Ke:Data curation, Formal analysis, Project administration, Software, Writing - review & editing.**Wei Guo**:Data curation, Methodology, Writing - original draft.**Shan Huang**:Investigation, Project administration, Writing - review & editing.**Yuxing Li**:Visualization, Writing - original draft, Validation.**Yuyan Guo**: Formal analysis, Investigation.**Xiaoxiao Liu**:Methodology, Software.**Yingying Jin**:Supervision.**Hongbing Ma**:Conceptualization, Resources, Funding acquisition, Supervision.

Declaration of competing interest

The authors declare that there is no conflict of interest.

Acknowledgments

We would like to thank Professor Yutaka Shimada at Hyogo College of Medicine for providing the KYSE30, KYSE140, KYSE150, KYSE170, KYSE180, KYSE410, and KYSE510 cell lines. We also thank the Shanghai OE Biotechnology Company (China) for providing arrays and primary data analysis. We thank Dr. Tao Yuandong (State Key Laboratory of Proteomics, National Center for Protein Sciences, Beijing. Beijing Proteome Research Center, Beijing Institute of Lifeomics) for his diligent proofreading of the manuscript and editing the figures. We thank Professor Zhao Xiaohang (State Key Laboratory of Molecular Oncology, Cancer Institute & Hospital, Chinese Academy of Medical Sciences & Peking Union Medical College, Beijing, China) for providing laboratory and Materials.

References

[1] A. Shibata, T. Matsuda, W. Ajiki, T. Sobue, Trend in incidence of adenocarcinoma of the esophagus in Japan, 1993-2001, Jpn. J. Clin. Oncol. 38 (7) (2008) 464–468.
[2] D.H. Ilson, Esophageal cancer chemotherapy: recent advances, Gastrointest Cancer Res 2 (2) (2008) 85–92.
[3] D.C. Lin, X.L. Du, M.R. Wang, Protein alterations in ESCC and clinical implications: a review, Dis. Esophagus 22 (1) (2009) 9–20.
[4] Y.J. Qi, W.X. Chao, J.F. Chiu, An overview of esophageal squamous cell carcinoma proteomics, J. Proteome 75 (11) (2012) 3129–3137.
[5] E. Garcia, C. Marcos-Gutierrez, M. del Mar Lorente, J.C. Moreno, M. Vidal, RYBP, a new repressor protein that interacts with components of the mammalian Polycomb complex, and with the transcription factor YY1, EMBO J. 18 (12) (1999) 3404–3418.
[6] K. Hisada, C. Sanchez, T.A. Endo, M. Endoh, M. Roman-Trufero, J. Sharif, H. Koseki, M. Vidal, RYBP represses endogenous retroviruses and preimplantation- and germ line-specific genes in mouse embryonic stem cells, Mol. Cell. Biol. 32 (6) (2012) 1139–1149.
[7] O. Ujhelly, V. Szabo, G. Kovacs, F. Vajda, S. Mallok, J. Prorok, K. Acsai, Z. Hegedus, S. Krebs, A. Dinnyes, M.K. Pirity, Lack of Rybp in mouse embryonic stem cells impairs cardiac differentiation, Stem Cells Dev. 24 (18) (2015) 2193–2205.
[8] M.K. Pirity, J. Locker, N. Schreiber-Agus, Rybp/DEDAF is required for early post-implantation and for central nervous system development, Mol. Cell. Biol. 25 (16) (2005) 7193–7202.
[9] R.D. Hanson, J.L. Hess, B.D. Yu, P. Ernst, M. van Lohuizen, A. Berns, N.M. van der Lugt, C.S. Shashikant, F.H. Ruddle, M. Seto, S.J. Korsmeyer, Mammalian Trithorax and polycomb-group homologues are antagonistic regulators of homeotic development, Proc. Natl. Acad. Sci. U. S. A. 96 (25) (1999) 14372–14377.
[10] L. Zheng, O. Schickling, M.E. Peter, M.J. Lenardo, The death effector domain-associated factor plays distinct regulatory roles in the nucleus and cytoplasm, J. Biol.

Chem. 276 (34) (2001) 31945–31952.
[11] W. Ma, X. Zhang, M. Li, X. Ma, B. Huang, H. Chen, D. Chen, Proapoptotic RYBP interacts with FANK1 and induces tumor cell apoptosis through the AP-1 signaling pathway, Cell. Signal. 28 (8) (2016) 779–787.
[12] A.A. Danen-van Oorschot, P. Voskamp, M.C. Seelen, M.H. van Miltenburg, M.W. Bolk, S.W. Tait, J.G. Boesen-de Cock, J.L. Rohn, J. Borst, M.H. Noteborn, Human death effector domain-associated factor interacts with the viral apoptosis agonist Apoptin and exerts tumor-preferential cell killing, Cell Death Differ. 11 (5) (2004) 564–573.
[13] W. Wang, J. Cheng, J.J. Qin, S. Voruganti, S. Nag, J. Fan, Q. Gao, R. Zhang, RYBP expression is associated with better survival of patients with hepatocellular carcinoma (HCC) and responsiveness to chemotherapy of HCC cells in vitro and in vivo, Oncotarget 5 (22) (2014) 11604–11619.
[14] Q. Zhao, W. Cai, X. Zhang, S. Tian, J. Zhang, H. Li, C. Hou, X. Ma, H. Chen, B. Huang, D. Chen, RYBP expression is regulated by KLF4 and Sp1 and is related to hepatocellular carcinoma prognosis, J. Biol. Chem. 292 (6) (2017) 2143–2158.
[15] X. Zhu, Z. Wang, X. Qiu, C. Tan, H. Yu, C. Bei, L. Qin, Y. Ren, S. Tan, Associations between single nucleotide polymorphisms in RYBP and the prognosis of hepatocellular carcinoma in a Chinese population, Carcinogenesis 38 (5) (2017) 532–540.
[16] X. Zhu, M. Yan, W. Luo, W. Liu, Y. Ren, C. Bei, G. Tang, R. Chen, S. Tan, Expression and clinical significance of PcG-associated protein RYBP in hepatocellular carcinoma, Oncol. Lett. 13 (1) (2017) 141–150.
[17] X. Dinglin, L. Ding, Q. Li, Y. Liu, J. Zhang, H. Yao, RYBP inhibits progression and metastasis of lung Cancer by suppressing EGFR signaling and epithelial-Mesenchymal transition, Transl. Oncol. 10 (2) (2017) 280–287.
[18] J. Jiang, Q. Gao, T. Wang, H. Lin, Q. Zhan, Z. Chu, R. Huang, X. Zhou, X. Liang, W. Guo, MicroRNA expression profiles of granulocytic myeloidderived suppressor cells from mice bearing Lewis lung carcinoma, Mol. Med. Rep. 14 (5) (2016) 4567–4574.
[19] S. Voruganti, F. Xu, J.J. Qin, Y. Guo, S. Sarkar, M. Gao, Z. Zheng, M.H. Wang, J. Zhou, B. Qian, R. Zhang, W. Wang, RYBP predicts survival of patients with non-small cell lung cancer and regulates tumor cell growth and the response to chemotherapy, Cancer Lett. 369 (2) (2015) 386–395.
[20] B.S. Taylor, N. Schultz, H. Hieronymus, A. Gopalan, Y. Xiao, B.S. Carver, V.K. Arora, P. Kaushik, E. Cerami, B. Reva, Y. Antipin, N. Mitsiades, T. Landers, I. Dolgalev, J.E. Major, M. Wilson, N.D. Socci, A.E. Lash, A. Heguy, J.A. Eastham, H.I. Scher, V.E. Reuter, P.T. Scardino, C. Sander, C.L. Sawyers, W.L. Gerald, Integrative genomic profiling of human prostate cancer, Cancer Cell 18 (1) (2010) 11–22.
[21] A. Krohn, A. Seidel, L. Burkhardt, F. Bachmann, M. Mader, K. Grupp, T. Eichenauer, A. Becker, M. Adam, M. Graefen, H. Huland, S. Kurtz, S. Steurer, M.C. Tsourlakis, S. Minner, U. Michl, T. Schlomm, G. Sauter, R. Simon, H. Sirma, Recurrent deletion of 3p13 targets multiple tumour suppressor genes and defines a distinct subgroup of aggressive ERG fusion-positive prostate cancers, J. Pathol. 231 (1) (2013) 130–141.
[22] P. Ulz, J. Belic, R. Graf, M. Auer, I. Lafer, K. Fischereder, G. Webersinke, K. Pummer, H. Augustin, M. Pichler, G. Hoefler, T. Bauernhofer, J.B. Geigl, E. Heitzer, M.R. Speicher, Whole-genome plasma sequencing reveals focal amplifications as a driving force in metastatic prostate cancer, Nat. Commun. 7 (2016) 12008.
[23] M.F. Buas, J.H. Rho, X. Chai, Y. Zhang, P.D. Lampe, C.I. Li, Candidate early detection protein biomarkers for ER+/PR+ invasive ductal breast carcinoma identified using pre-clinical plasma from the WHI observational study, Breast Cancer Res. Treat. 153 (2) (2015) 445–454.
[24] T.C. Kenny, H. Schmidt, K. Adelson, Y. Hoshida, A.P. Koh, N. Shah, J. Mandeli, J. Ting, D. Germain, Patient-derived interstitial fluids and predisposition to aggressive sporadic breast Cancer through collagen remodeling and inactivation of p53, Clin. Cancer Res. 23 (18) (2017) 5446–5459.
[25] H. Zhou, J. Li, Z. Zhang, R. Ye, N. Shao, T. Cheang, S. Wang, RING1 and YY1 binding protein suppresses breast cancer growth and metastasis, Int. J. Oncol. 49 (6) (2016) 2442–2452.
[26] M. Lando, M. Holden, L.C. Bergersen, D.H. Svendsrud, T. Stokke, K. Sundfor, I.K. Glad, G.B. Kristensen, H. Lyng, Gene dosage, expression, and ontology analysis identifies driver genes in the carcinogenesis and chemoradioresistance of cervical cancer, PLoS Genet. 5 (11) (2009) e1000719.
[27] M. Lando, S.M. Wilting, K. Snipstad, T. Clancy, M. Bierkens, E.K. Aarnes, M. Holden, T. Stokke, K. Sundfor, R. Holm, G.B. Kristensen, R.D. Steenbergen, H. Lyng, Identification of eight candidate target genes of the recurrent 3p12-p14 loss in cervical cancer by integrative genomic profiling, J. Pathol. 230 (1) (2013) 59–69.
[28] G. Li, C. Warden, Z. Zou, J. Neman, J.S. Krueger, A. Jain, R. Jandial, M. Chen, Altered expression of polycomb group genes in glioblastoma multiforme, PLoS One 8 (11) (2013) e80970.
[29] D.O. Minchenko, S.V. Danilovskyi, I.V. Kryvdiuk, N.A. Hlushchak, O.V. Kovalevska, L.L. Karbovskyi, O.H. Minchenko, Acute L-glutamine deprivation affects the expression of TP53-related protein genes in U87 glioma cells, Fiziol. Zh. 60 (4) (2014) 11–21.
[30] E. Andersson, C. Sward, G. Stenman, H. Ahlman, O. Nilsson, High-resolution genomic profiling reveals gain of chromosome 14 as a predictor of poor outcome in ileal carcinoids, Endocr. Relat. Cancer 16 (3) (2009) 953–966.
[31] O. Nilsson, Profiling of ileal carcinoids, Neuroendocrinology 97 (1) (2013) 7–18.
[32] Fillmore Helen, Li Gang, Warden Charles, Zou Zhaoxia, Neman Josh, S. Krueger Joseph, Jain Alisha, Jandial Rahul, Chen Mike, Altered expression of Polycomb group genes in Glioblastoma Multiforme, PLoS One 8 (11) (2013) e80970.
[33] Y. Shimada, M. Imamura, T. Wagata, N. Yamaguchi, T. Tobe, Characterization of 21 newly established esophageal cancer cell lines, Cancer 69 (2) (1992) 277–284.
[34] W. Li, G. Hou, D. Zhou, X. Lou, Y. Xu, S. Liu, X. Zhao, The roles of AKR1C1 and AKR1C2 in ethyl-3,4-dihydroxybenzoateinduced esophageal squamous cell carcinoma cell death, Oncotarget (2016), https://doi.org/10.18632/oncotarget.7775.
[35] Y. Xu, L. Zhou, J. Huang, F. Liu, J. Yu, Q. Zhan, L. Zhang, X. Zhao, Role of Smac in determining the chemotherapeutic response of esophageal squamous cell carcinoma, Clin. Cancer Res. 17 (16) (2011) 5412–5422.
[36] D.R. Rhodes, J. Yu, K. Shanker, N. Deshpande, R. Varambally, D. Ghosh, T. Barrette, A. Pandey, A.M. Chinnaiyan, ONCOMINE: a cancer microarray database and integrated data-mining platform, Neoplasia 6 (1) (2004) 1–6.
[37] N. Hu, R.J. Clifford, H.H. Yang, C. Wang, A.M. Goldstein, T. Ding, P.R. Taylor, M.P. Lee, Genome wide analysis of DNA copy number neutral loss of heterozygosity (CNNLOH) and its relation to gene expression in esophageal squamous cell carcinoma, BMC Genomics 11 (576) (2010).
[38] H. Su, N. Hu, H.H. Yang, C. Wang, M. Takikita, Q.H. Wang, C. Giffen, R. Clifford, S.M. Hewitt, J.Z. Shou, A.M. Goldstein, M.P. Lee, P.R. Taylor, Global gene expression profiling and validation in esophageal squamous cell carcinoma and its association with clinical phenotypes, Clin. Cancer Res. 17 (9) (2011) 2955–2966.
[39] R.A. Sclafani, T.M. Holzen, Cell cycle regulation of DNA replication, Annu. Rev. Genet. 41 (2007) 237–280.
[40] J.T. Yeeles, T.D. Deegan, A. Janska, A. Early, J.F. Diffley, Regulated eukaryotic DNA replication origin firing with purified proteins, Nature 519 (7544) (2015) 431–435.
[41] S. Chen, X. Chen, G. Xie, Y. He, D. Yan, D. Zheng, S. Li, X. Fu, Y. Li, X. Pang, Z. Hu, H. Li, W. Tan, J. Li, Cdc6 contributes to cisplatin-resistance by activation of ATR-Chk1 pathway in bladder cancer cells, Oncotarget 7 (26) (2016) 40362–40376.
[42] Y.H. Kim, Y.J. Byun, W.T. Kim, P. Jeong, C. Yan, H.W. Kang, Y.J. Kim, S.C. Lee, S.K. Moon, Y.H. Choi, S.J. Yun, W.J. Kim, CDC6 mRNA expression is associated with the aggressiveness of prostate Cancer, J. Korean Med. Sci. 33 (47) (2018) e303.
[43] W. Jiang, Y. Yu, J. Liu, Q. Zhao, J. Wang, J. Zhang, X. Dang, Downregulation of Cdc6 inhibits tumorigenesis of osteosarcoma in vivo and in vitro, Biomed. Pharmacother. 115 (2019) 108949.
[44] Y. Hu, L. Wang, Z. Li, Z. Wan, M. Shao, S. Wu, G. Wang, Potential prognostic and diagnostic values of CDC6, CDC45, ORC6 and SNHG7 in colorectal Cancer, Onco Targets Ther 12 (2019) 11609–11621.
[45] R. Arrigoni, S.L. Alam, J.A. Wamstad, V.J. Bardwell, W.I. Sundquist, N. Schreiber-Agus, The Polycomb-associated protein Rybp is a ubiquitin binding protein, FEBS Lett. 580 (26) (2006) 6233–6241.
[46] D. Chen, J. Zhang, M. Li, E.R. Rayburn, H. Wang, R. Zhang, RYBP stabilizes p53 by modulating MDM2, EMBO Rep. 10 (2) (2009) 166–172.
[47] M. Li, S. Zhang, W. Zhao, C. Hou, X. Ma, X. Li, B. Huang, H. Chen, D. Chen, RYBP modulates stability and function of Ring1B through targeting UBE3A, FASEB J. 33 (1) (2019) 683–695.
[48] M.A.M. Ali, H. Strickfaden, B.L. Lee, L. Spyracopoulos, M.J. Hendzel, RYBP is a K63-ubiquitin-chain-binding protein that inhibits homologous recombination repair, Cell Rep. 22 (2) (2018) 383–395.
[49] S. Schlisio, T. Halperin, M. Vidal, J.R. Nevins, Interaction of YY1 with E2Fs, mediated by RYBP, provides a mechanism for specificity of E2F function, EMBO J. 21 (21) (2002) 5775–5786.